Electrochemical Properties of Melamine-Based Carbon

Denisa Hulicova*, Masaya Kodama, Junya Yamashita, Yasushi Soneda, Hiroaki Hatori
Energy Storage Material Research Group, Institute for Energy Utilization, National Institute of Advanced Industrial Science and Technology, AIST West, 16-1 Onogawa, Tsukuba, Ibaraki 305-8569, Japan

**Corresponding author e-mail address:denisa-hulicova@aist.go.jp*

Introduction

In recent years supercapacitors have attracted a serious attention as the alternative power sources. Nowadays, activated carbon is the most frequently used as the electrode materials for supercapacitors [1,2]. The storage of electric charges is a purely non-Faradaic and the accumulation of ionic charges occurs on a double-layer at the electrode/electrolyte interface [3]. Large specific surface area and the porosity of activated carbon are the basic requirements for achieving the quick formation of double-layer resulting to a high power density and long durability of these supercapacitors termed also the electric double-layer capacitors (EDLC). The capacitive behavior of carbon materials can be further improved by the presence of active species that contribute to the total specific capacitance by the pseudocapacitive effect [3]. Active species such as metal oxides [4] or conducting polymers [5,6] can be reversibly oxidized/reduces over the potential range of operation. The presence of heteroatoms and functional groups in a carbon matrix change the electron/donor characteristics of the carbon electrode material [7]. It was assumed that nitrogen functionalities change the electron donor/acceptor characteristics of carbon depending on the type of the groups formed between the nitrogen and carbon atoms [8].
This report discusses the electrochemical performance of supercapacitors made of carbon material with a moderate amount of nitrogen atoms embedded in a carbon matrix. For the first time capacitors were manufactured from a melamine-derived carbon. Because the melamine resin contains 45 wt% of nitrogen we believed it would be a promising candidate for the synthesis of nitrogen rich carbon electrode material for supercapacitors. Melamine was polymerized in the interlayer spaces of fluorine mica and the pure nitrogen enriched carbon was obtained after mica removal. Mica was expected to introduce a layer-like structure and a certain degree of order into the resulted carbon material. The electrochemical characteristics of prepared samples are discussed with respect to their porosities and elemental compositions.

Experimental

Melamine (2,3,6-triamino-1,3,5-triazine, Kanto Chemicals Co., Inc., purity 98%) and expandable fluorine mica (synthesized at AIST Kyushu) were used as the starting materials. Melamine/mica composite was prepared by the polymerization of melamine in the interlayer spaces of expandable fluorine mica in formaldehyde in the ratio of

melamine/ mica/ formaldehyde = 3/ 1/ 8 by weight. Polymerization took place at pH~ 9.1 and temperatures of 80 ºC for 0.5h under the intensive stirring. After drying at 60 ºC in a conventional oven, samples were carbonized in an infrared furnace under the nitrogen atmosphere and temperatures of 650 ºC, 750 ºC, 800 ºC, 850 ºC, and 1000 ºC; heating rate 10 ºC/min and holding period of 1h. Each sample was also stabilized in air at 250 ºC for 4h prior to carbonization.

Samples subjected to no-stabilization process are hereafter denoted as Me650, Me750, Me800, Me850, and Me1000. Their stabilized counterparts are denoted as Me650s, Me750s, Me800s, Me850s, and Me1000s.

The elemental analysis was done by a conventional CHN combustion method. X-ray photoelectron spectroscopy (XPS, ESCA 5600, Ulvac-Phi, Inc. Japan) was also used in the surface analyses of the samples. Mg Kα line (15 kV, 30 mA, 400 W) was used as an X-ray source and the C_{1s} peak position was set at 284.6 eV and taken as an internal standard. The peak separation of N_{1s} core level peaks was estimated by least squares using Gaussian-Lorentzian product function with the Grams/386 software.

The surface morphology of Me750 and Me750s was observed by field-emission scanning electron microscope (JEOL S-4700, operated at 1.5 kV).

To characterize the pore structure, nitrogen adsorption/desorption measurement at 77 K was conducted using the Belsorp18, Bel Japan, Inc. instrument. The α_s plots were created by the use of standard adsorption isotherm of the nonporous carbon black (Mitsubishi No.32). The surface areas, micropores and mesopores volumes as well as micropores and mesopores widths were then determined by subtracting pore effect (SPE) method.

Pellets for the electrochemical measurement were prepared by mixing the carbonized sample with carbon black (Mitsubishi chemicals, Inc.) and polytetrafluoroethylene binder (PTFE, Mitsui Dupont Fluorochemicals, 7A-J, Inc.). The ratio of sample: CB: PTFE was 80: 10: 10 wt%. Then the ammonium hydrocarbonate was added in a ratio of sample: NH_4HCO_3 = 1: 1 by weight. NH_4HCO_3 was expected to form small pores in a pellet during its decomposition at the drying process (110 ºC in vacuum) and such pores should help the electrolyte diffusion. The final pellet weight was set on ca 20 mg. Cyclic voltammmetry (CV) and galvanostatic charge/discharge cycling (GC) were employed in the evaluation of double-layer capacitance for each sample. Both CV and GC experiments were carried out at room temperature and the nitrogen bubbling in a standard three-compartment cell, when platinum foil and Ag/AgCl were used as the counter and the reference electrode, respectively. 1M H_2SO_4 was used as an electrolyte. GC with the current loading of 20 mAg^{-1} was conducted in a multichanel VMP potentiostat/galvanostat (Multi-channel potentiostats/galvanostats VMP-80, Princeton Applied research) in the potential range from -0.2 V to 0.5 V versus Ag/AgCl.

CV was performed under the following conditions: potential scan rate of 0.1 mVs^{-1} and potential range of 0-0.5 V.

Results and Discussion

Figure 1 shows the FE-SEM photographs of Me750 and Me750s. The layer like structure proving that the melamine polymerized in the interlayer space of mica can be observed in both samples though Me750 appears to be denser and less porous.

The results on N/C ratio evaluated from the CHN elemental analysis, N/C ratio determined from XPS analysis, and the carbonization yield of each and individual sample are shown in Table 1. Nitrogen content reasonably decreases with the heat-treatment temperature for both the non-stabilized and stabilized samples. It is also observed that the stabilized samples, contain generally much higher amount of nitrogen when compare with the non-stabilized ones. This indicates that the stabilization process was very effective in "trapping" the nitrogen atoms in a carbon matrix and therefore Me1000s still contained a moderate amount of nitrogen (N/C= 0.13) despite the relatively high heat-treatment temperature. The carbon yields (Table 1) become lower with the heat-treatment temperature in non-stabilized samples, e.g. carbon yields of Me650, Me1000 are 30.37% and 20.96%, respectively. Stabilized samples provide higher carbonization yield as it increases to 41.58% and 30.38 wt% for Me650s and Me1000s, respectively.

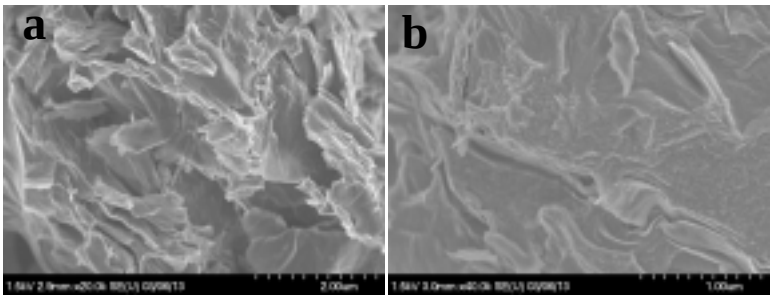

Fig.1. FE-SEM photographs of Me750 (a) and Me750s (b). A layer-like structure can be observed in both the samples although Me750s is denser.

Table 1. N/C ratios of non-stabilized and stabilized samples evaluated from CHN and XPS; and carbon yields of all samples.

Sample	N/C_{CHN}	N/C_{XPS}	Yield [wt%]
Me650	0.37	0.22	30.37
Me750	0.24	0.20	25.71
Me800	0.24	---	24.20
Me850	0.20	0.21	23.26
Me1000	0.08	0.11	20.86
Me650s	0.45	0.45	41.58
Me750s	0.43	0.34	39.40
Me800s	0.41	---	36.57
Me850s	0.32	0.25	34.89
Me1000s	0.13	0.14	30.38

The porous nature of all samples was further investigated by N_2 adsorption/desorption measurement. Surface areas (SA), total pore volumes (V_{total}), micropore volumes (V_{micro}), mesopore volumes (V_{meso}), micropore widths (w_{micro}), and mesopore widths (R_{meso}) of all samples are listed in Table 2. Taking into account the total amount of nitrogen adsorbed, it can be said that the porosities in all samples are not developed much. It is a reasonable conclusion as no activation process has been used. Among the non-stabilized samples, Me750 adsorbs the highest amount of nitrogen and therefore it is a sample with the highest porosity (SA= 442 m^2g^{-1}). The adsorption of N_2 was observed at low relative pressure due to the micropore-filling effect. Then the adsorption gradually increases in the region of middle P/P_s and further in the region of high pressure, such as >0.8 P/P_s. This kind of adsorption behavior can be attributed to the capillary condensation of nitrogen in the mesopores or macropores and multilayer adsorption of mesopores or macropores. As for the stabilized samples, they are less

porous when compare with their non-stabilized counterparts. Me750s is again the sample with the highest SA among the stabilized samples (SA= 256 m^2g^{-1}), however the surface area is reduced significantly. As for the Me1000s SA decreases dramatically to 17 m^2g^{-1} and similar reduction in the surface areas can be observed for each stabilized sample. The reason for that is thought to be the stabilization process at which the sample melted and shrunken and therefore the release of gases during the carbonization process could not form pores into same extend as in the non-stabilized samples.

Table 2. Surface areas, total pore volumes, micropores volumes, mesopores volumes, mean micropores widths, and mesopores widths for non-stabilized and stabilized samples. All values are calculated by SPE method.

Sample	$SA_{\alpha s}$ [m^2g^{-1}]	V_{total} [mlg^{-1}]	V_{micro} [mlg^{-1}]	V_{meso} [mlg^{-1}]	w_{micro} [nm]	R_{meso} [nm]
Me650	260	0.24	0.08	0.16	0.72	8.7
Me750	442	0.38	0.13	0.25	0.73	5.9
Me800	345	0.41	0.09	0.31	0.95	4.0
Me850	248	0.35	0.06	0.29	0.73	6.8
Me1000	86	0.21	0.01	0.20	0.80	6.5
Me650s	138	0.25	0.03	0.22	0.58	12.1
Me750s	256	0.32	0.07	0.25	0.74	7.5
Me800s	202	0.27	0.05	0.22	0.78	6.0
Me850s	120	0.24	0.02	0.22	0.71	6.9
Me1000s	17	0.17	---	0.15	---	4.3

Figure 2 shows the results on N_{1s} peak analysis of all samples. The fitting of N_{1s} for all samples shows the existence of three contributions at binding energies of 398.7, 400.9, and 402.7 eV. These peaks can be assigned to pyridine (398.5± 0.2 eV), quaternary (401.2± 0.2 eV), and oxidized nitrogen (402.9± 0.2 eV), respectively [9,10]. The amount of quaternary nitrogen increases with the HTT indicating chemical change of nitrogen groups during the heat treatment. Thus the peripheral pyridinic nitrogen has been transformed to the quaternary nitrogen located within the graphene sheets through the condensation reaction. The proportion of pyridinic N in stabilized samples is generally higher. This indicates that the stabilization process affected the

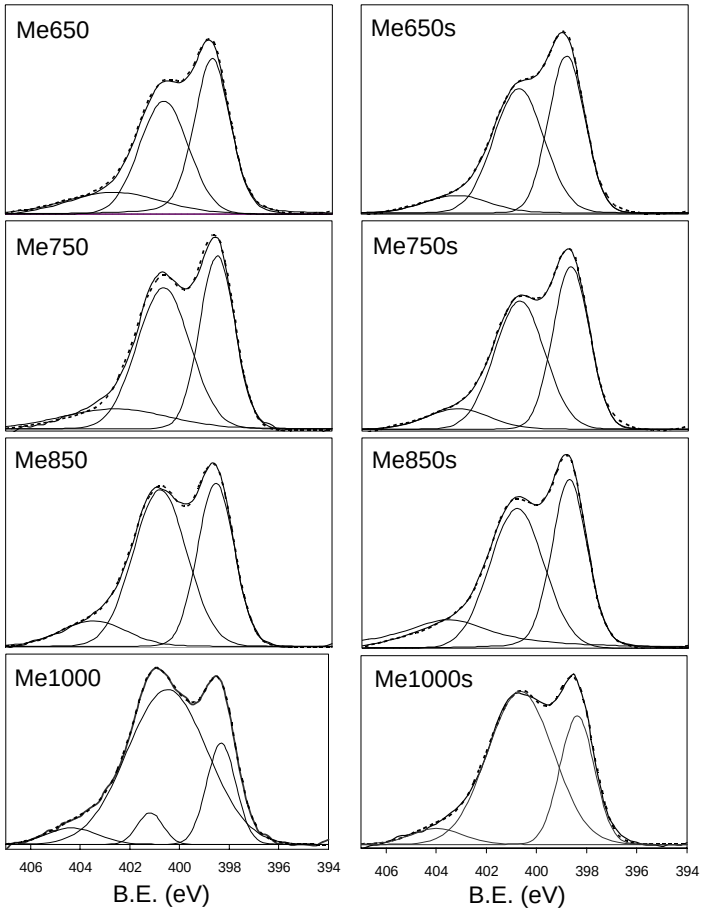

Fig.2. N_{1s} peak analyses of stabilized and non-stabilized samples.

Table 3. Specific gravimetric capacitances (C_g) and specific capacitances per surface area (C_{SA}) of all samples. Calculation are done from the discharge process of the third cycle in the potential range of 0.2-0.1V; surface areas are estimated by SPE method.

	Me650	Me750	Me800	Me850	Me1000	Me650s	Me750s	Me800s	Me850s	Me1000s
C_g [Fg^{-1}]	141.1	204.8	198.8	157.4	47.92	128.2	200.1	185.6	195.9	62.24
C_{SA} [Fm^{-2}]	0.54	0.46	0.57	0.63	0.55	0.93	0.78	0.92	1.63	3.66

condensation reaction of pyridinic groups and that the nitrogen species of stabilized samples are located preferably at the edges of graphene sheets.

The specific gravimetric capacitances (C_g) and specific capacitances per surface areas (C_{SA}) evaluated from the GC measurements are summarized in Table 3. Concerning the C_g of non-stabilized samples, it is remarkable that the values are unexpectedly high with respect to the low porosities. It can be seen that the capacitance increases with HTT reaching the maximum of 204.8 Fg^{-1} for Me750. This sample has the highest specific surface area among the non-stabilized samples (SA= 442 m^2g^{-1}) and high ratio of nitrogen (N/C= 0.24). However, with further increasing of the carbonization temperature the capacitance decreases down to the minimum of 47.92 Fg^{-1} for Me1000. This is the sample with the lowest specific surface area (SA= 86 m^2g^{-1}) and the lowest ratio of nitrogen (N/C= 0.08). The gravimetric capacitances of stabilized samples are close to their non-stabilized counterparts despite the remarkably lower surface areas. Again sample heat-treated at 750 ºC ($Me750_s$) is the sample with the highest SA (256 m^2g^{-1}) and the best gravimetric capacitive performance (C_g= 200.1 Fg^{-1}). As expected, $Me1000_s$ is almost non-porous sample with the SA= 17 m^2g^{-1} and the poorest gravimetric capacitance (C_g= 62.24 Fg^{-1}).

As for the C_{SA} of non-stabilized samples the values of all samples are similar or very close. Me750 is even the sample with the lowest value of C_{SA} among the non-stabilized samples (0.46 Fm^{-2}) and Me850 is a sample with the best capacitive performance (0.63 Fm^{-2}). C_{SA} values of the stabilized samples are generally higher than those for the non-stabilized ones. It is reasonable as the stabilized samples are less-porous while providing high values of C_g. Among the stabilized samples Me750s is again a sample with the lowest C_{SA} (0.78 Fm^{-2}), however it is still a higher value if compare with it's non-stabilized counterpart. The best capacitive performance per surface area s measured for Me1000s (3.66 Fm^{-2}). This is a sample with almost no porosity (SA= 17 m^2g^{-1}) and the lowest amount of nitrogen (N/C= 0.14). For the samples presented in this work not only the double-layer capacitance but also the pseudocapacitive effect should be considered because of the presence of incorporated nitrogen in a serious amount. It was suggested that the pyridinic nitrogen at the periphery of graphene layer provides a pair of electrons introducing the electron donor properties to the layer [10]. XPS studies clearly show the presence of pyridinic and quaternary nitrogen in all samples while the pyridinic nitrogen ratios are higher in stabilized samples. These nitrogen species are located at the easily accesible edges of graphene layers and therefore one can reasonably assume that the protons were attracted to the electrode surface and the pseudocapacitive electrosorption occurred. This may be a reason for the good capacitive properties of

stabilized samples with very poor porosities but with the higher ratios of pyridinic nitrogen. Figure 3 shows the example voltammograms for Me750 and Me750s. The voltammogram for Me750 is almost square suggesting the dominant pure electrostatic attraction. However, a slight slope in the region of proton electrosorption can be observed. This indicates some deviations from the ideal double-layer capacitors. Such deviations become more significant in Me750s when voltammograms for this sample is not square and the slope is easily recognized. Me750 is the sample with the certain porosity and therefore it is possible that the pure electrostatic sorption of ions occurred simultaneously with the pseudocapacitive attraction between the protons and nitrogen species of carbon. On the other hand, the surface area of Me750s is lower and the nitrogen content is higher. Therefore it can be assumed that the contribution of pseudocapacitance to the total capacitance is higher in Me750s than in Me750. The voltammograms of other samples have similar shapes indicating the same behavior, i.e. the dominant pseudocapacitive attraction in stabilized samples.

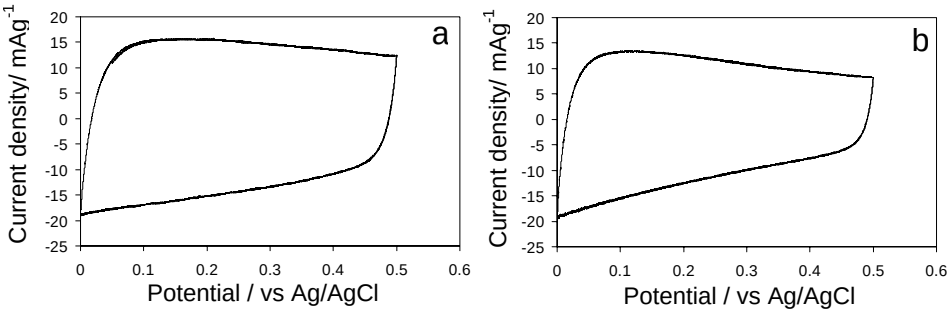

Fig.3. Cyclic voltammograms of the capacitors manufactured from Me750 (c) and Me750s (d).

Conclusions

Novel electrochemical capacitors were manufactured from melamine-based carbons prepared by a template method using fluorine mica as template. The nitrogen content in stabilized samples was higher compare to their non-stabilized counterparts while the surface area was reduced significantly at stabilization process. XPS revealed that the main nitrogen species presented were pyridinic, quaternary, and oxidized nitrogen. The ratio of peripheral pyridinic nitrogen in stabilized samples was higher and it was claimed to be a reason for the high values of capacitance of these samples. It was suggested that the pseudocapacitive attraction between the protons and the pyridinic nitrogen occuerd leading to a good performance of capacitors manufactured from melamine-based carbon.

References

[1] S. Shiraishi, H. Kurihara, L. Shi, T. Nakayama, A. Oya, Electric Double-layer Capacitance of Meso/Macroporous Activated Carbon Fibers Prepared by the Blending Method. J. Electrochemical Society 2002;149 (7): A855-A861

[2] A. Lewandowski, M. Zajder, E. Frackowiak, F. Beguin. Supercapacitor based on activated carbon and polyethylene oxide–KOH–H_2O polymer electrolyte. Electrochimica Acta 2001;46:2777-2780
[3] B.E. Conway. Electrochemical Supercapacitors: Scientific Fundamentals and Technological Applications. Kluwer-Plenum Press New York 1999
[4] H. Kim, B.N. Popov. Characterization of hydrous ruthenium oxide/carbon nanocomposite supercapacitors prepared by a colloidal method. J. Power Sources 2002;104: 52-61
[5] W.Chen, T. Wen, H. Teng. Polyaniline-deposited Porous Carbon Electrode for Supercapacitor. Electrochimica Acta 2003;48;641-649
[6] N.D. Ingram, A.J. Pappin, F. Delalande, D. Poupard, G. Terzulli. Development of electrochemical capacitors incorporating processable polymer gel electrolytes. Electrochimica Acta 1998;43:10601-1605
[7] Y.P. Wu, E. Rahm, R. Holze. Effects of heteroatoms on electrochemical performance of electrode for lithium ion batteries. Electrochimica Acta 2002;47:3491-3507
[8] Y. Wu, S. Fang, Y. Jiang. Carbon anode materials based on melamine resin. J. Materials Chemistry 1998;8 (10):2223-2227
[9] E. Raymundo-Pinero, D. Cazorla-Amoros, A. Linares-Solano, J. Find, U. Wild, R. Schlogl. Structural characterization of N-containing activated carbon fibers prepared from a low softening point petroleum pitch and a melamine resin. Carbon 2002;40:597-608
[10] M. Koh, T. Nakajima. Adsorption of aromatic compounds on C_xN-coated activated carbon. Carbon 2000;38:1947-1954